Cancer Management and Research

Dovepress

open access to scientific and medical research

Open Access Full Text Article

ORIGINAL RESEARCH

ZNF488 is an independent prognostic indicator in nasopharyngeal carcinoma and promotes cell adhesion and proliferation via collagen IV/FAK/AKT/Cyclin D1 pathway

This article was published in the following Dove Press journal:
Cancer Management and Research

Dan Zong
Ning Jiang
Jian-Hua Xu
De-Jun Wang
Huan-Feng Zhu
Li-Rong Wu
Cheng Chen
Li Yin
Xia He

Jiangsu Cancer Hospital, Jiangsu Institute of Cancer Research, The Affiliated Cancer Hospital of Nanjing Medical University, Nanjing, Jiangsu Province 210009, People's Republic of China

Background: ZNF488 acts as an oncogene which promotes cell invasion and endows tumor cells stem cell capacity in nasopharyngeal carcinoma (NPC), but its correlation with clinicopathologic characteristics and patients' survival in NPC remain undefined.

Methods: In this study, 158 cases of confirmed NPC were subjected to immunohistochemistry staining for evaluating endogenous expression. Kaplan–Meier method and log-rank test were used to estimate the survival rates. The relationship between ZNF488 and clinicopathological characteristics was statistically calculated by chi-squared test, univariate and multivariate analysis. In addition, adhesion assay, MTT and colony formation assays were performed for measuring adhesion and proliferation capacity. Cell cycle analysis via flow cytometry was conducted to explore cell cycle distribution. Western blot was used to detect pathway protein levels, and the pFAK (Y397) kit was used for focal adhesion kinase (FAK) activation.

Results: We demonstrated that high expression of ZNF488 was significantly correlated with locoregional failure (P=0.018) and distant metastasis (P=0.001). Patients with high ZNF488 expression had poorer overall survival (P<0.001), loco-regional recurrence-free survival (P<0.001), distance metastasis-free survival (P<0.001) and progression-free survival (P<0.001) than those with low ZNF488 group. Multivariate analysis showed that ZNF488 expression was an independent prognostic indicator for predicting NPC patients' survival (HR, 3.314; 95% CI, 1.489–7.386; P=0.003). Additionally, ZNF488-induced collagen IV/FAK/AKT to enhance adhesion ability meanwhile led to the upregulation of Cyclin D1 to facilitate cell proliferation through promoting cell cycle progression and inhibition of apoptosis through caspase-independent way.

Conclusion: These results reveal that ZNF488, as an independent prognostic indicator, promotes cell adhesion and proliferation through collagen IV/FAK/AKT/Cyclin D1 pathway in NPC.

Keywords: nasopharyngeal carcinoma, ZNF488, proliferation, FAK/AKT/Cyclin D1, prognostic biomarker

Correspondence: Xia He
Jiangsu Cancer Hospital, Jiangsu Institute of Cancer Research, The Affiliated Cancer Hospital of Nanjing Medical University, 42 Baiziting Road, Xuanwu District, Nanjing, Jiangsu Province 210009, People's Republic of China
Tel +861 360 145 8518
Fax +86 258 328 3560
Email hexiabm@163.com

Introduction

Nasopharyngeal carcinoma (NPC) has a distinctive geographic distribution with high incidence in Southeast Asia.[1] NPC patients usually receive radiotherapy or concurrent chemo-radiotherapy, following with adjuvant chemotherapy.[2] Due to the chemo- and radio-sensitive characteristics, this treatment approaches result in cure of most patients, as results showing in our cancer center.[3,4] However, NPC patients at the same clinical

submit your manuscript | www.dovepress.com
DovePress
http://doi.org/10.2147/CMAR.S200001

stage often have different clinical outcomes due to distant metastasis or locoregional failure.[5] Although many studies have recognized viral, smoking, genetic makeup and carcinogen exposure as risk factors, the molecular mechanism of genesis and heterogeneity in NPC are poorly understood. It is of great value to find valuable diagnostic markers and understand the molecular mechanism for novel therapeutic targeting. Much research have explored the development of innovative strategies of the hallmarks for preventing distant relapse. For instance, it has been demonstrated that EGFR is correlated with clinicopathological characteristics and prognosis in many cancers.[6] Clinical applications of anti-EGFR antibodies (cetuximab) in combination with intensity-modulated radiotherapy (IMRT) have been found to be more effective than radiotherapy alone for both locoregional control and overall survival (OS) in patients with locoregionally advanced nasopharyngeal carcinoma, with low gastrointestinal reactions, hepatotoxicity and bone marrow suppression.[7]

Zinc Finger Protein 488 (ZNF488) is a Kruppel-like zinc finger transcription factor, which is thought to be an oligodendrocyte-specific transcriptional repressor that cooperates with Olig2 to promote oligodendrocyte differentiation in myelin regeneration and repair in demyelinating diseases.[8,9] Recently, ZNF488 was demonstrated to be an oncogene, which promoted invasion and tumorigenesis through Wnt/β-catenin/GSK3β pathway to induce epithelial mesenchymal transition (EMT) in NPC.[10] However, the clinical significance and other biological function of ZNF488 in NPC have not been thoroughly investigated.

In this article, we elucidate the potential value of ZNF488 expression as a biomarker for predicting patients' prognosis in NPC. We also show that overexpression of ZNF488 promotes cell adhesion and proliferation. Mechanistically, ZNF488-induced collagen IV/FAK upregulation can activate AKT to enhance adhesion ability, meanwhile leads to cell proliferation through upregulation of Cyclin D1 and inhibition of caspase-dependent apoptosis.

Materials and methods

Nasopharyngeal patients and clinical tissue specimens

One hundred and fifty-eight cases of paraffin-embedded NPC tissues, which were obtained from Jiangsu Cancer Hospital, were subjected to immunohistochemistry. All cases were definitely diagnosed with NPC of non-keratinising squamous cell carcinoma (WHO 2). All were with prior written consent of patients and approval of the Institutional Clinical Ethics Review Board while in accordance with the Declaration of Helsinki. The histological grade and stage of tumors were classified according to the criteria of the 7th eition of the American Joint Committee on Cancer (AJCC) cancer staging system 7.

Radiotherapy

The nasopharyngeal and neck tumor volumes of all patients were treated using radical radiotherapy based on IMRT for the entire course. Gross tumor volumes were defined based on MR, CT and PET/CT imaging before induced chemotherapy (IC). Target volumes were delineated slice-by-slice on treatment planning CT scans. Intensity-modulated radiotherapy with 7~9 field fixed angle was adopted. The specific prescription dose was as follows: planned target area (PTVnx) of primary focus (GTVnx), 66~75 Gy for 32~34 times. Cervical lymph node metastasis (GTVnd) PTVnd, 66~70 Gy, 32~34 times. PTV2 of CTV1 (high-risk area) and CTV2 (low-risk area) were 60.0 Gy and 50.4 Gy, respectively. Dose limits for organs at risk: maximum dose of brainstem, optic nerve and optic chiasm <54 Gy, maximum dose of temporal lobe <69 Gy, temporomandibular joint <60Gy, maximum dose of spinal cord <45 Gy, average dose of parotid gland <30 Gy, average dose of bulbus oculi <35 Gy, maximum dose of crystalline lens <6 Gy. All targets were treated simultaneously using the simultaneous integrated boost technique.

Chemotherapy

During the study, institutional guidelines recommended IMRT alone for stage I NPC and IMRT combined with chemotherapy for stage II–IVa NPC. For IVa NPC, after assessment of tumor volume, many people may receive IC before IMRT. Two regimes of IC were frequently used: cisplatin (75 mg/m^2) with docetaxel (80 mg/m^2), and cisplatin (60 mg/m^2) plus docetaxel (60 mg/m^2) with 5-fluorouracil (600–750 mg/m^2 per day for 5 days) every 3 weeks for 2–4 cycles. Concurrent chemotherapy consisted of cisplatin (75 mg/m^2) with docetaxel (80 mg/m^2) every 3 weeks for 2–3 cycles or cisplatin (40 mg/m^2) weekly for 5–7 cycles. Adjuvant chemotherapy included cisplatin (75 mg/m^2) with docetaxel (80 mg/m^2) every 3 weeks for 2–4 cycles just for high-risk patients or residual lesions. When possible, salvage treatments (such as intracavitary brachytherapy, surgery, or chemotherapy) were provided for documented relapse or persistent disease.

Cell culture

Human NPC cells HNE1 and CNE1 were maintained in RPMI-1640 ((Life Technologies) supplemented with 10% fetal bovine serum (Gibco). All these cell lines have been demonstrated by STR profile. The HEK 293FT cell line was maintained in DMEM (Invitrogen) supplemented with 10% fetal bovine serum, which was originally obtained from the American Type Culture Collection.[11]

Plasmids and generation of stably transfected cell line

The construction of plasmids and stable ZNF488-overexpressing and control cell lines were described as previously.[10]

Immunofluorescence (IF) staining

We plated cells on multiwall coverslips to 80% confluence. After washing in PBS, cells were fixed in freshly prepared 4% polyphosphate formaldehyde for 10 mins and incubated in PBS three times. 10 min with PBS containing 0.5% Triton X-100, 2*5 min with PBS and blocked in 5% BSA for 30 min. Cells were incubated with primary antibodies ZNF488 (abcam) overnight at 4°C. After washing with PBS, slides were incubated with Alexa Fluor* 488 goat anti-rabbit IgG antibodies (Invitrogen) for 1 h, counterstained with DAPI (Sigma) to visualize nuclei, followed by Laser Scanning Confocal Microscope (Olympus).

Adhesion assay

Coat 96-well plate with Matrigel (BD Biosciences) at 37°C for 2 hrs. Leave some wells uncoated as negative controls. Cells were counted to 5×10^5/mL, and add 50 μL cells in each well. Incubate in CO_2 incubator at 37°C for 30 mins. Shake the plate at 2000 rpm for 10 s and wash with washing buffer 3 times. Fix with 4% paraformaldehyde for 15 mins and wash with washing buffer 3 times. Formazan was solubilized by adding 100 μL/well of DMSO (Sigma-Aldrich) and OD was measured at 570 nm using a microplate reader (Thermo).

FAK activation

The pFAK (Y397) kit was purchased from Invitrogen (Carlsbad) and we conducted the test according to the manufacturer's protocol. The OD was measured at 450 nm using a microplate reader. The readout was plotted against standard control.

Western blot

Protein samples were electrophoresed on 6–12% SDS polyacrylamide gel and transferred to polyvinylidene difluoride membrane (PVDF, Merck Millipore). The PVDF was blocked in 5% nonfat milk and incubated with primary antibodies against ZNF488 (Abcam), Collagen IV (Abcam), integrin α5 (Abcam), p-FAK (Y397) (Cell Signaling Technology (CST)), FAK (CST), ERK 1/2(Cell Signaling Technology), p-ERK1/2 (CST), Akt (CST), p-Akt (CST), Cyclin D1 (Abcam), Cyclin D2 (Abcam), Cyclin E (C-19) (Santa Cruz), α-tubulin (CST) and Cleaved caspase 9 p10 (Santa Cruz) overnight at 4°C. The PVDF membrane was incubated with anti-mouse or rabbit IgG secondary antibodies. α-tubulin served as the loading control. The band on the PVDF membrane was observed using an electrochemiluminescence kit (Pierce).

MTT assay

Cells were seeded in 96-well plates at a density of 1,000 cells per well. Cells were stained with 20 μL of MTT (Sigma-Aldrich) for 4 hrs. The medium was removed, and formazan was solubilized by adding 100 μL/well of DMSO (Sigma-Aldrich) and the OD was measured at 570 nm using a microplate reader (Thermo).

Colony formation assay

Cells were seeded in six-well plates at a density of 500 cells per well and cultured for 7–12 days. Colonies were fixed with 4% paraformaldehyde solution, stained with 0.5% crystal violet, and counted under an inverted microscope (Canon).

Cell cycle analysis via flow cytometry analysis

Cells were harvested, washed with cold PBS, and fixed in 70% ethanol. The cells were washed, re-suspended in PBS, and incubated with propidium iodide (Sigma-Aldrich) and RNase (Sigma-Aldrich) solution at room temperature for 30 mins in the dark. The stained cells were analyzed using flow cytometer (Beckman Coulter), and the percentage of cells in each cell cycle phase was calculated. The proliferation index (PI) was calculated as (S +G2/M)/(G1+S +G2/M) and the S-phase cell fraction as S/(G1+S +G2/M).

Immunohistochemistry (IHC) staining

Formalin-fixed, paraffin-embedded NPC samples were cut into 4-μm-thick slices. Slices were baked for 3 hrs at 58°C,

deparaffinized in xylenes and rehydrated with graded alcohol to distilled water, immersed in 3% hydrogen peroxide for 10 mins to block endogenous peroxidase activity at room temperature, and boiled the slices for antigen retrieval in Citrate Antigen Retrieval Solution (pH=6.0) for 5 mins in a high pressure cooker. After this retrieval solution cools down to room temperature, slices were incubated with diluted rabbit polyclonal anti-ZNF488 antibody (Sigma) overnight at 4°C in a moist chamber. After being washed in PBS, Tween-20 (PBST) is added and the slices were incubated with secondary antibody for 30 mins at 37°C and washed in PBST, followed by a 1-min staining in 3,3-diaminobenzidine. One negative control was performed with a normal nasopharyngeal epithelial tissue, and the other was obtained by replacing the primary antibody with a normal rabbit IgG.

Evaluation of IHC

The immunoreactivities were scored by two pathologists blinded to the clinical parameters. Tumor cell percentage and staining intensity were assessed, respectively. Tumor cell percentage was scored as follows: negative or less than 10% positive tumor cells, 0; 10–25% positive tumor cells, 1; 26–60% positive tumor cells, 2; more than 60% positive tumor cells, 3. staining intensity was classified as follows: no staining, 0; weak staining, 1; moderate staining, 2; strong staining, 3. We multiplied the two individual parameters to get an immunoreactivity score ranging from 0 to 9. An optimal cutoff value for high or low expression was selected with log-rank test statistical analysis to OS. For ZNF488, the optimal cutoff value was 5.0 to define tumor with low or high expression.

Follow-up

The follow-up duration was measured from the first day of treatment to the day of last examination or death. Patients were followed up every 3 months for the first 3 years after radiotherapy, every 6 months for the fourth to fifth years, and annually thereafter until death. Follow-up included physical examination, hematology and biochemistry profiles, Epstein–Barr virus (EBV)-DNA,MRI, chest CT scan, abdominal, ultrasonography, and whole-body bone scanning using single photon emission computed tomography. PET/CT was pformed when necessary. Locoregional recurrence-free survival was defined as the time from initiation of therapy to first locoregional failure. Progression-free survival (PFS) was defined as the time from initiation of therapy to failure or death from any cause, whichever occurred first. Distant metastasis-free survival (DMFS) was defined as the time from initiation of therapy to first distant failure. OS was defined as the time from the initiation of therapy to death from any cause.

Statistical analysis

Data are presented as the mean ± SD, and differences between groups were analysed using Student's t-test or chi-squared test. The Kaplan-Meier method and log-rank test were used to estimate survival rates. Multivariate survival analysis was performed on all parameters that were found to be significant on univariate analysis using the Cox regression model. All statistical analyses were performed with SPSS 18.0 software, and *P*-values of <0.05 were considered statistically significant.

Result

ZNF488 expression and the clinical characteristics of NPC patients

We detected ZNF488 protein levels in 158 paraffin-embedded NPC tissues by immunohistochemistry. Representative staining pictures of ZNF488 in NPC tissues were shown in Figure 1A-F. ZNF488 was highly expressed in 57 of the 158 (36.1%) NPC patients examined. Patients with high ZNF488 expression showed more locoregional failure (P=0.018) and distant metastasis (*P*=0.001) (Table 1). There were no significant associations between ZNF488 expression and patient gender, age, T stage, N stage, M stage and clinical TNM stage (Table 1).

ZNF488 expression and survival of NPC patients

The Kaplan-Meier analysis and log-rank test were used to calculate the effects of ZNF488 on patients' survival. Our results indicated that patients with high ZNF488 expression had poorer OS ($P<0.001$), locoregional recurrence-free survival ($P<0.001$), distance metastasis-free survival ($P<0.001$) and PFS ($P<0.001$) rates than patients with low ZNF488 expression (Figure 1, G-J). The cumulative 5-year survival rate was 70/101 (69.3%) in the low-ZNF 488-expression group, whereas it was only 30/57 (52.6%) in the high expression group.

Because of relatively small sample size, univariate and multivariate analyses using Cox regression model were applied to exclude the potential interfering factors. Some reported factors, including age, gender, T classification, N classification, radiation dose,

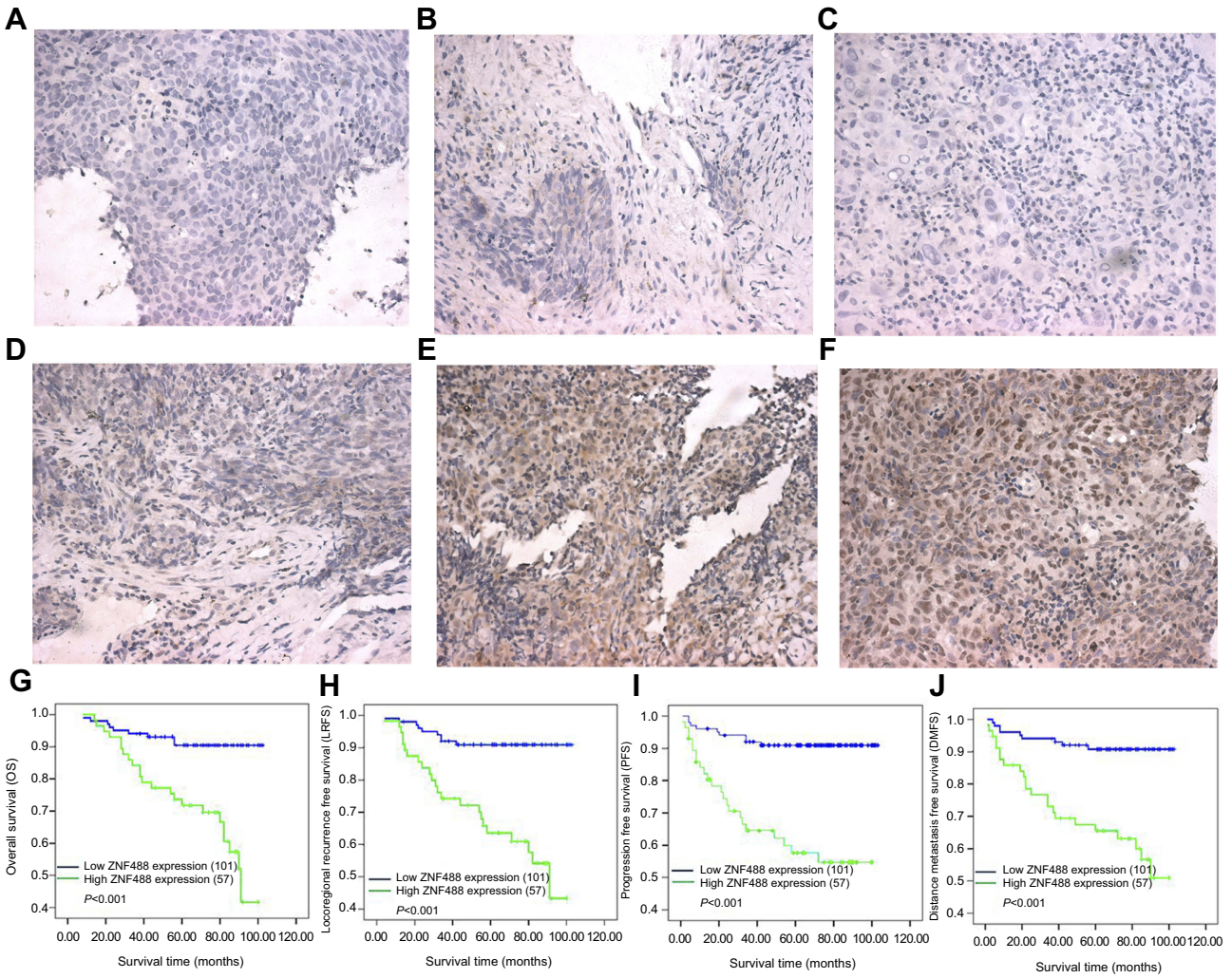

Figure 1 High expression of ZNF488 is correlated with poor clinical outcomes. (**A**) Negative ZNF488 staining in nasopharyngeal epithelium tissue, (**B**) negative ZNF488 staining in NPC tissue with normal rabbit IgG, (**C**) negative staining of ZNF488, (**D**) weak staining, (**E**) moderate staining, (**F**) strong staining (magnification 400×). (**G**) Overall survival, (**H**) locoregional recurrence-free survival. (**I**) Distant-metastasis-free survival. (**J**) Progression-free survival.

chemotherapy, distant metastasis, and loco-regional failure,[12] were incorporated for analysis. Univariate analyses indicated that ZNF488 expression, T stage, radiotherapy dose, distant metastasis, and locoregional failure were significant predictors for patients' OS (P<0.05, Table 2). Since ZNF488 expression and other clinicopathologic features were significant in univariate analysis, these variables were further examined in multivariate analysis. Multivariate analysis showed that ZNF488 expression was evaluated as an independent risk factor for adverse prognosis (HR: 3.314; 95% confidence interval: 1.489–7.386; P=0.003, Table 2). Additionally, T stage (HR:2.886; 95% confidence interval: 1.155–7.210; P=0.023, Table 2), radiation dose (HR:4.197; 95% confidence interval: 1.746–10.085; P=0.001, Table 2), distant metastasis (HR: 6.962; 95% confidence interval: 3.316–14.618; P<0.001), and loco-regional failure (HR: 2.806; 95% confidence interval: 1.345–5.853; P=0.006) were independent prognostic indicators in this study (Table 2).

Effects of ZNF488 on adhesion ability and FAK signaling pathway

Before functional experiments, we verified the transfection efficiency in stable cells by IF staining and Western blot. (Figure 2A, B). During cell culture, we observed that ZNF488-overexpressing stable cell lines presented much more attachment capability as the time of enzymatic digestion in ZNF488-overexpressing cells was longer than the control. These results led us to test whether ZNF488 regulates cell adhesion. Adhesion assays showed that overexpression of ZNF488

Table 1 Clinical characteristics of NPC patients according to high and low ZNF488 expression

Characteristics	ZNF488 expression		*P*-value
	Low or none, n=101(%)	High, n=57(%)	
Age			1.000
<50	49 (48.5)	27 (47.4)	
≥50	52 (51.5)	30 (52.6)	
Gender			0.704
Male	74 (73.3)	44 (77.2)	
Female	27 (26.7)	13 (22.8)	
TNM stage			1.000
I–II	3 (3.0)	1 (1.80)	
III– IV	98 (97.0)	56 (98.2)	
T stage			0.175
T1– T2	44 (43.6)	18 (31.6)	
T3– T4	57 (56.4)	39 (68.4)	
N stage			0.833
N0–N1	18 (17.8)	11 (19.3)	
N2–N3	83 (82.2)	46 (80.7)	
M stage			0.057
M0	100 (99.1)	53 (99.3)	
M1	1 (0.01)	4 (0.07)	
Locoregional failure			**0.018**
Yes	16 (15.8)	85 (84.2)	
No	18 (31.6)	39 (68.4)	
Distant metastasis			**0.001**
Yes	11 (10.9)	16 (28.1)	
No	90 (89.1)	31 (71.9)	

Notes: Two-sided *P*-values were calculated using Pearson's chi-square test or continuity correction to evaluate the significance of the correlations. Bold values indicate statistical significance (*P*<0.05).

Table 2 Univariate analysis and multivariable cox regression analyses of ZNF488 expression levels and overall survival

Variable	Univariate analysis			Multivariate analysis		
	HR	95%CI	*P*-value	HR	95%CI	*P*-value
ZNF488 expression (high vs low)	4.602	2.124–9.969	**<0.001**	3.314	1.489–7.386	**0.003**
Age (<50 vs ≥50 years)	0.915	0.447–1.874	0.484			
Gender (female vs. male)	0.644	0.380–1.818	0.831			
T stage (3–4 vs1-2)	3.320	1.365–8.079	**0.008**	2.886	1.155–7.210	**0.023**
N stage (2–3 vs 0–1)	1.191	0.660–2.155	0.110			
Radiation dose (<70 Gy vs ≥70Gy)	2.565	1.095–6.008	**0.030**	4.197	1.746–10.085	**0.001**
Chemotherapy (no vs yes)	1.082	0.440–2.661	0.557			
Distant metastasis (yes vs no)	8.077	4.008–16.278	**<0.001**	6.962	3.316–14.618	**<0.001**
Locoregional failure (yes vs no)	2.873	1.428–5.778	**0.003**	2.806	1.345–5.853	**0.006**

Note: Bold values indicate statistical significance (*P*<0.05).

increased the number of adherent cells both in HNE1 and CNE1 (Figure 2C). FAK signaling is crucial in mediating cell adhesion and migration.[13] Indeed, overexpression of ZNF488 increased the phosphorylation of FAK without expressional change on total FAK (Figure 2E) as well as in vitro pFAK activation assay (Figure 2D). The results

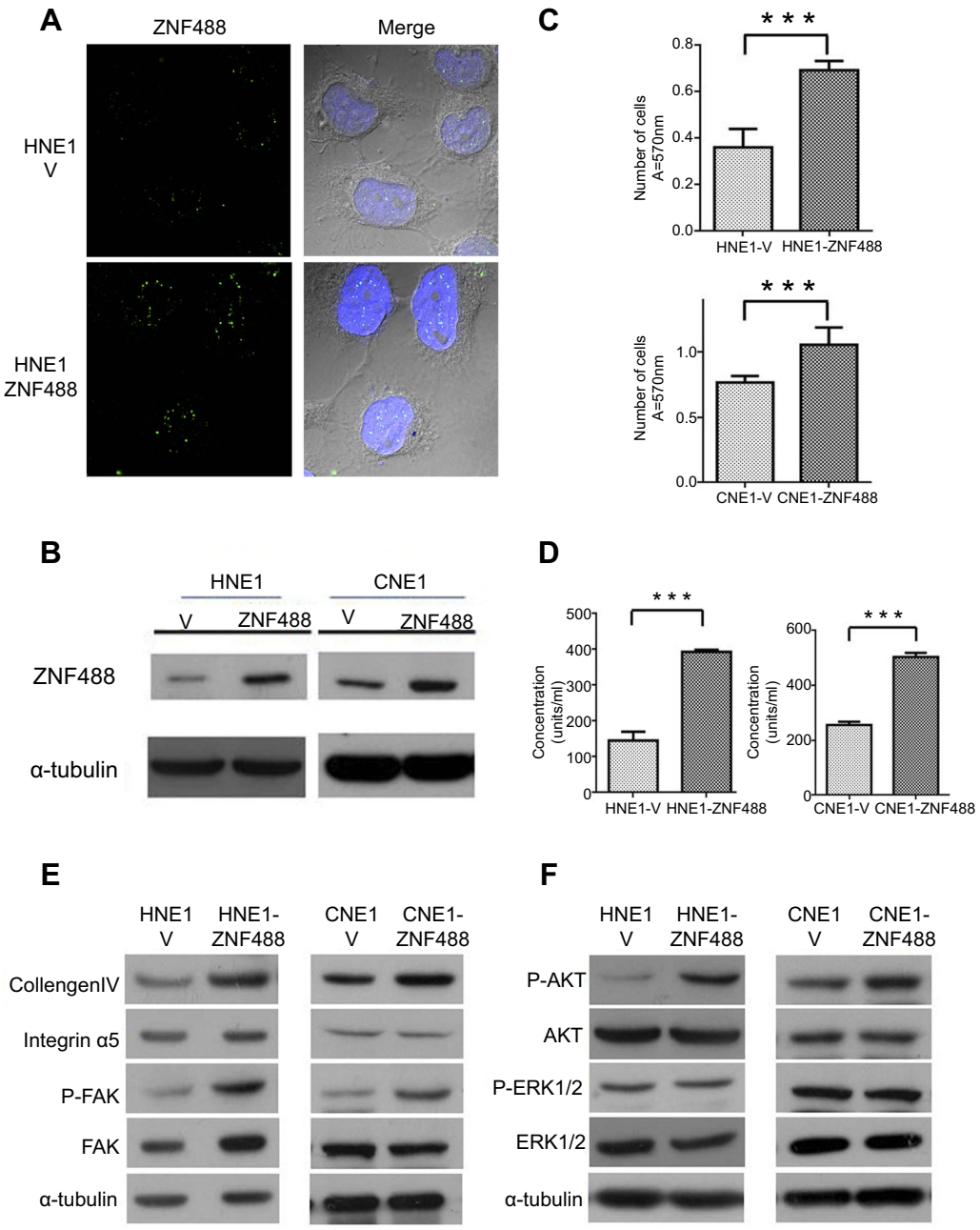

Figure 2 Effects of ZNF488 on adhesion ability and FAK signaling pathway. (**A**) Immunofluoresce for ZNF488 detection. (**B**) Western blot to detect ZNF488 protein level in both HNE1 and CNE1 ZNF488 overexpression stable cell lines and vector. (**C**) Adhesion assay in HNE1 and CNE1. (**D**) FAK activation assay to detect the activity of pFAK (Y397). (**E**) Western blot to detect collagen IV, integrin α5, FAK and p-FAK(Y397). (**F**) Western blot to detect ERK 1/2, p-ERK1/2, Akt and p-Akt. *** $P<0.001$.

suggested that FAK signaling pathway might be implicated in ZNF488-mediated cell adhesion.

To explore the underlying mechanism of ZNF488 on cell adhesion, molecules related to ECM and FAK signaling pathway were analyzed. ZNF488-overexpressing cells had a higher level of collagen IV compared with the control without change of integrin α5 (Figure 2E).The level of p-AKT in ZNF488-overexpressing group increased significantly, while total levels of AKT, p-ERK1/2, and ERK1/2 did not change (Figure 2F). These results suggest that the effect of ZNF488 on cell adhesion may be via modulation of collagen IV/FAK/AKT pathway.

Effects of ZNF488 on cell proliferation

Stiff ECM often gives rise to aberrant proliferation through pathological cellular responses.[14] To explore the effect of ZNF488 on cell proliferation in HNE1 and CNE1, MTT and colony formation assays were performed. Growth curves

showed that overexpression of ZNF488 grew faster than control cells (Figure 3A, $P<0.05$). Colony formation assay showed that overexpression of ZNF488 exhibited more colonies than the control (Figure 3B, $P<0.001$). Together, ZNF488 indeed enhance proliferation in NPC.

Effect of ZNF488 on cell cycle distribution and cyclin D1

To investigate the potential effect of ZNF488 on cell cycle, we conducted flow cytometry experiment to know the status of cell cycle in ZNF488-overexpressing and control cells. In order to synchronize the phase of cell cycle, we starved the cells for 36 hrs to block cells in G0/G1 phase. Cell cycle distribution was shown in Figure 4A-B, cell populations in the G1, S, and G2/M phases of the cell cycle presented differences between ZNF488-overexpressing and control cells after releasing 24 hrs. Proliferative index (PI) is a measure of the number of cells in a tumor which can be an indicator for proliferation. The PI of HNE1-V 0H, HNE1-V 24H, HNE1-ZNF488 0H, and HNE1-ZNF488 24H was 25.61%, 32.18%, 30.2%, and 40.33%, respectively. After 24-hr culture, the added PI was 10.13% in HNE1-ZNF488 cells compared with 6.57% in HNE1-V. Consistent with result in HNE1, the added PI was 22.90% in CNE1-ZNF488 compared with 15.81% in CNE1-V (Figure 4C). Overexpression of ZNF488 showed elevated PI and S-phase cell fraction (Figure 4D), suggesting overexpression of ZNF488 prompted cell cycle progression to enhance proliferation in NPC.

As overexpression of ZNF488 prompted cell cycle progression, we explored whether ZNF488 had an effect on cell cycle regulatory genes. Overexpression of ZNF488 strongly upregulated the expression of cyclin D1 without affecting

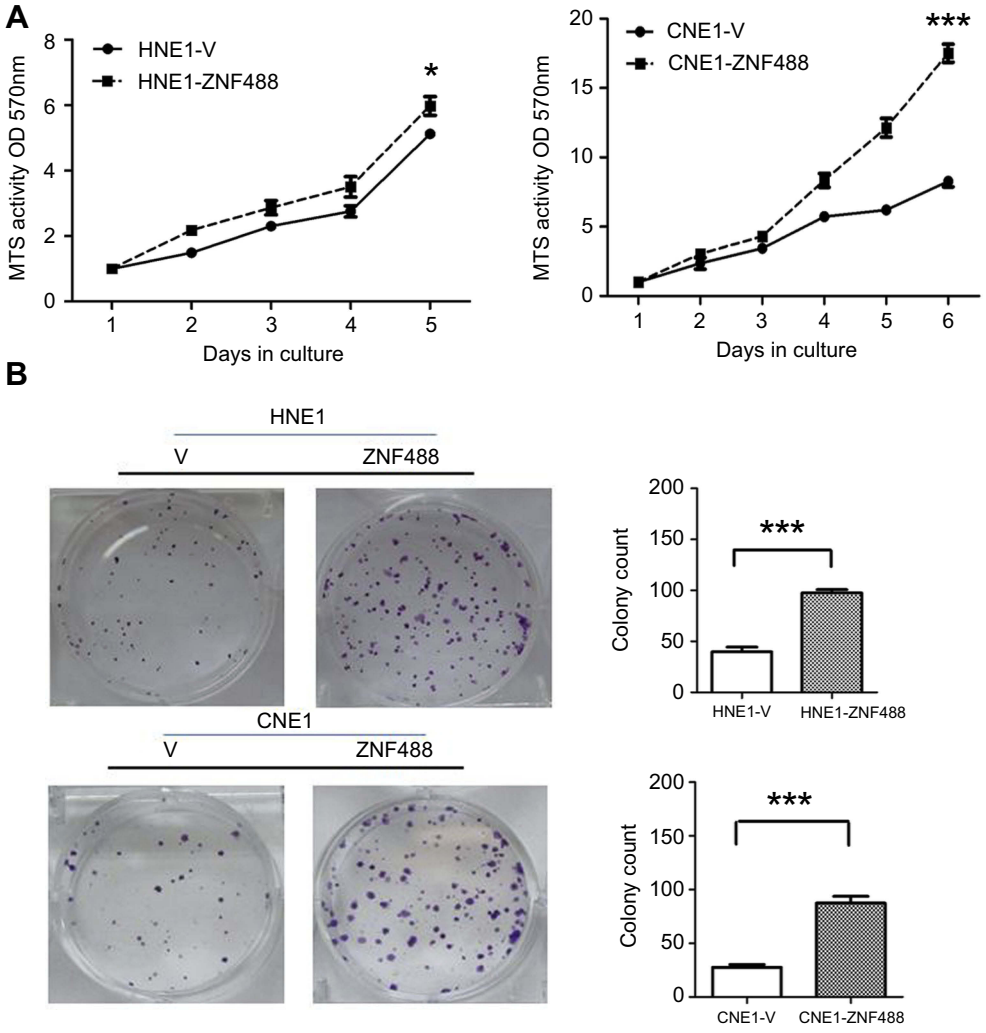

Figure 3 Effects of ZNF488 on cell proliferation. (**A**) The growth curves of MTT assays in both HNE1 and CNE1. (**B**) Colony formation assays were conducted. * $P<0.05$; *** $P<0.001$.

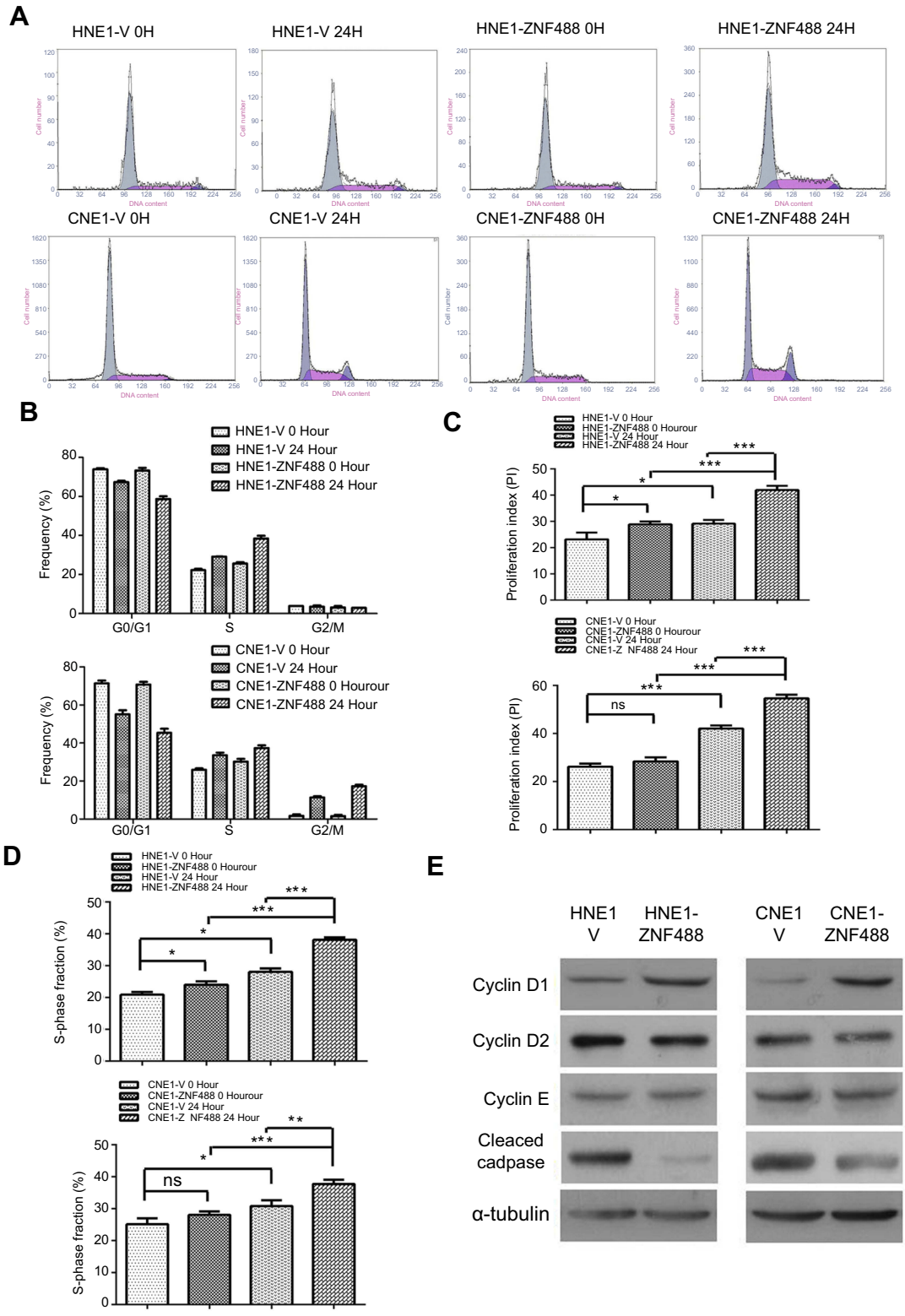

Figure 4 Effect of ZNF488 on cell cycle distribution and Cyclin D1. **(A)** Cell cycle analysis with flow cytometry were performed in HNE1 and CNE1. **(B)** Results of cell cycle analysis with histogram. **(C)** Proliferation index of each group. **(D)** S-phase fraction of each group. **(E)** Western blot to detect the protein level of cyclin D1, Cyclin D2, Cyclin E (C-19), and cleaved caspase 9 p10. NS, no significance. * $P<0.05$, ** $P<0.01$, *** $P<0.001$.

cyclin D2 and cyclin E (Figure 4E). In addition, FAK regulates the caspase-independent apoptotic pathway to resist cell death.[15] Supporting this notion is that overexpression of ZNF488 significantly inhibited apoptosis in HNE1 and CNE1, as indicated by a decreased level of activated apoptotic marker–cleaved-caspase 9 (Figure 4E). These observations suggest that ZNF488-induced FAK/AKT led to the upregulation of cyclin D1 to promote cell cycle progression and the inhibition of apoptosis through the caspase-independent way.

Discussion

NPC is an epithelial malignancy arising from the superior portion of the pharynx, extending from the upper surface of the soft palate to the base of the skull. The process involved in the development of NPC most is intermingled with latent EBV infection and often is of high incidence of lymph node and distant metastasis with familial and somatic genetic and epigenetic variations. ZNF488 acts as an oncogene which increases NPC invasion and endowes tumor stem cell ability through EMT by activating Wnt/β-catenin/GSK3β pathway.[10] However, little was known about the correlation between clinical factors and ZNF488 expression and other biological functions.

In this paper, we thought to explore the function of ZNF488 more deeply and investigate the potential value of ZNF488 expression as a biomarker in NPC. FAK is thought to be a crucial factor, and disorder of FAK and its downstream cellular signaling are key intermediators of cancer malignance such as invasion, adhesion, proliferation, and metastasis.[16,17] As a key component of sensing stiffness to extracellular matrix (ECM), FAK mediates a complicated network of signaling pathways for the interaction of cells with its physical environment to remodel ECM.[18,19] ECM substrates, including collagen I/IV, laminin, integrin, and fibronectin, supporting cell structure, mediate cell adhesion.[20] Collagens are the most abundant proteins that constitute fibers and peri-cellular basement membranes, and researchers have demonstrated that collagens are crucial not only for tissue structures but also for the regulation of cellular signaling transduction.[21] Some studies verified that FAK, as one of the downstream effector proteins, can be rapidly autophosphorylated (Tyrosine-397, Y397) following stiffness changes with cell adhesion to collagen.[22,23] Importantly, activated FAK signaling pathways are extensive, which can also activate Ras/MAPK pathway and transduce signal activation to PI3K/AKT, which contributes to cyclin D synthesis and caspase-dependent cell death.[17,24,25]

Our results showed that patients with high ZNF488 expression presented significant associations with locoregional failure and distant metastasis; meanwhile, they presented poorer overall, locoregional recurrence-free, distance metastasis-free, and PFS rates than patients with low expression. Based on the improvement of radiation technique, concurrent-adjuvant chemotherapy, and targeting preparation, the 5-year OS rate was approximately 80%.[26,27] But in our study, 5-year OS rate was 63.3%, which might be the result of unbalanced clinical stage that the majority (97.5%) of enrolled NPC patients have loco-regionally advanced disease. In addition, ZNF488 might act as an independent prognostic factor in NPC patients. We also confirmed that radiation dose, T stage, distant metastasis, and loco-regional failure were independent predictive factors, which were consistent with previous studies.[28] These results suggest that ZNF488 expression status can serve as a valuable prognostic biomarker to stratify NPC patients into different risk groups and further guide individual therapy choices.

In addition to its biological significance in invasion and tumorigenesis in NPC, ZNF488 plays an important role in cell adhesion. Cell adhesion, especially adhesion to ECM, is vital to cell invasion and metastasis.[29] ECM remodeling is important for cell adhesion, which is rich in collagen, laminin, integin, and fibronectin.[30,31] The previous study has demonstrated that ZNF488 can upregulate fibronectin.[10] Supportively, ZNF488 could increase collagen IV to facilitate cell adhesion, which indicated that ZNF488 could contribute to ECM remodeling. FAK is reported to involve the ECM remodeling and cell adhesion,[32] and activated FAK can activate a cascade of phosphorylation to trigger signaling pathways, such as MAPK and PI3K/AKT.[33] FAK can activate PI3K/AKT, which contributes to cyclin D synthesis and caspase-dependent cell death.[17,24,25] FAK autophosphorylation (Y397) leads to cell adhesion and stiffness changes, which can also recruits 85KD subunit of phosphatidylinositol-3-kinase (PI3K). The activated PI3K stimulates the PKB/Akt to transmembrane through its PH domain, resulting in PKB/Akt phosphorylation. The active PKB/Akt promotes proliferation through phosphorylation and prevention of pro-apoptotic proteins.[34] The activated apoptotic pathway causes mitochondrial outer membrane opening to release a number of apoptotic proteins, which leads to caspase-9 activation and ultimately apoptosis.[34,35] Accumulating studies have demonstrated that FAK can enhance proliferation and inhibit apoptosis in a caspase-dependent way.[13] Our results showed that

overexpression of ZNF488 promoted cell proliferation with FAK activation. Overexpression of ZNF488 had elevated PI and S-phase cell fraction, indicating that ZNF488 promoted cell cycle progression in HNE1 and CNE1. In addition, overexpression of ZNF488 increased the abundance of cyclin D1and inhibited the apoptotic marker Cleaved caspase 9. As studies have verified that FAK transduced ECM stiffness into intracellular stiffness, increased cyclin D1 expression,[36] and FAK regulated the caspase-independent apoptotic pathway to resist cell death.[15] We proposed that the upregulation of cyclin D1 and inhibition of cleaved caspase 9 in ZNF488-overexpressing cells were followed by FAK activation. Therefore, our results indicate a possible mechanism that ZNF488-induced collagen IV upregulation via FAK activity could enhance the activation of AKT to enhance adhesion ability, which also led to the upregulation of cyclin D1 and inhibition of apoptosis for cell proliferation.

In conclusions, our results indicated that ZNF488 can serve as a valuable prognostic biomarker to stratify NPC patients into different risk groups and predict patient survival. Overexpression of ZNF488 enhances cell adhesion via collagen IV/FAK/AKT pathway, which upregulates cyclin D1 to promote cell cycle progression and inhibits apoptosis through the caspase-independent way. But our study has some limitations. The poor prognosis is in part related to the development of therapy resistance during conservative treatment, whether it involves in the acquisition of chemo/radio-resistance is not clear. Thus, more works will be in need to unveil the effect of ZNF488 on the therapeutic response in NPC.

Acknowledgments

This study was partly supported by the National Natural Science Foundation grants of China (81702693) and (81602381), China Postdoctoral Science Foundation (NO. 2017M621679), and Grants of Jiangsu Cancer Hospital (ZN201604) and (ZQ201504) , The Young Talents program of Jiangsu Cancer Hospital.

Disclosure

The authors report no conflicts of interest in this work.

References

1. Liu F, Jin T, Liu L, et al. The role of concurrent chemotherapy for stage II nasopharyngeal carcinoma in the intensity-modulated radiotherapy era: A systematic review and meta-analysis. *PLoS One*. 2018;13(3):e0194733. doi:10.1371/journal.pone.0194733
2. Feng Y, Cao C, Hu Q, et al. Prognostic value and staging classification of lymph nodal necrosis in nasopharyngeal carcinoma after intensity-modulated radiotherapy. *Cancer Res Treat*. 2018. doi:10.4143/crt.2018.595
3. Wu LR, Jiang XS, Song X, et al. Comparing the efficacy of induction-concurrent with concurrent-adjuvant chemotherapy in locoregionally advanced nasopharyngeal carcinoma: a propensity score matching analysis. *Oncotarget*. 2017;8(45):79953–79963. doi:10.18632/oncotarget.20389
4. Wu LR, Liu YT, Jiang N, et al. Ten-year survival outcomes for patients with nasopharyngeal carcinoma receiving intensity-modulated radiotherapy: an analysis of 614 patients from a single center. *Oral Oncol*. 2017;69:26–32. doi:10.1016/j.oraloncology.2017.03.015
5. Li Z, Li N, Shen L. MAP2K6 is associated with radiation resistance and adverse prognosis for locally advanced nasopharyngeal carcinoma patients. *Cancer Manag Res*. 2018;10:6905–6912. doi:10.2147/CMAR.S184689
6. Lin M, You R, Liu YP, et al. Beneficial effects of anti-EGFR agents, Cetuximab or Nimotuzumab, in combination with concurrent chemoradiotherapy in advanced nasopharyngeal carcinoma. *Oral Oncol*. 2018;80:1–8. doi:10.1016/j.oraloncology.2018.03.002
7. Peng H, Tang LL, Liu X, et al. Anti-EGFR targeted therapy delivered before versus during radiotherapy in locoregionally advanced nasopharyngeal carcinoma: a big-data, intelligence platform-based analysis. *BMC Cancer*. 2018;18(1):323. doi:10.1186/s12885-018-4242-8
8. Wang SZ, Dulin J, Wu H, et al. An oligodendrocyte-specific zinc-finger transcription regulator cooperates with Olig2 to promote oligodendrocyte differentiation. *Development*. 2006;133(17):3389–3398. doi:10.1242/dev.02522
9. Soundarapandian MM, Selvaraj V, Lo UG, et al. Zfp488 promotes oligodendrocyte differentiation of neural progenitor cells in adult mice after demyelination. *Sci Rep*. 2011;1:2. doi:10.1038/srep00002
10. Zong D, Yin L, Zhong Q, et al. ZNF 488 Enhances the invasion and tumorigenesis in nasopharyngeal carcinoma via the Wnt signaling pathway involving epithelial mesenchymal transition. *Cancer Res Treat*. 2015
11. An W, Yao S, Sun X, et al. Glucocorticoid modulatory element-binding protein 1 (GMEB1) interacts with the de-ubiquitinase USP40 to stabilize CFLARL and inhibit apoptosis in human non-small cell lung cancer cells. *J Exp Clin Cancer Res*. 2019;38(1):181. doi:10.1186/s13046-019-1182-3
12. Xu JH, Guo WJ, Bian XH, et al. A comparative study of locoregionally advanced nasopharyngeal carcinoma treated with intensity modulated irradiation and platinum-based chemotherapy. *Cancer Radiother*. 2013;17(4):297–303. doi:10.1016/j.canrad.2013.03.006
13. Lin TY, Hsu HY. Ling Zhi-8 reduces lung cancer mobility and metastasis through disruption of focal adhesion and induction of MDM2-mediated Slug degradation. *Cancer Lett*. 2016. doi:10.1016/j.canlet.2016.03.018
14. Schrader J, Gordon-Walker TT, Aucott RL, et al. Matrix stiffness modulates proliferation, chemotherapeutic response, and dormancy in hepatocellular carcinoma cells. *Hepatology*. 2011;53(4):1192–1205. doi:10.1002/hep.24108
15. Hwang YJ, Lee EJ, Kim HR, et al. Molecular mechanisms of luteolin-7-O-glucoside-induced growth inhibition on human liver cancer cells: G2/M cell cycle arrest and caspase-independent apoptotic signaling pathways. *BMB Rep*. 2013;46(12):611–616.
16. Gerard C, Goldbeter A. The balance between cell cycle arrest and cell proliferation: control by the extracellular matrix and by contact inhibition. *Interface Focus*. 2014;4(3):20130075. doi:10.1098/rsfs.2013.0075
17. Mitra SK, Hanson DA, Schlaepfer DD. Focal adhesion kinase: in command and control of cell motility. *Nat Rev Mol Cell Biol*. 2005;6(1):56–68. doi:10.1038/nrm1549
18. Zheng Y, Lu Z. Paradoxical roles of FAK in tumor cell migration and metastasis. *Cell Cycle*. 2009;8(21):3474–3479. doi:10.4161/cc.8.21.9846

19. Lohberger B, Kaltenegger H, Weigl L, et al. Mechanical exposure and diacerein treatment modulates integrin-FAK-MAPKs mechanotransduction in human osteoarthritis chondrocytes. *Cell Signal*. 2018
20. Stendahl JC, Kaufman DB, Stupp SI. Extracellular matrix in pancreatic islets: relevance to scaffold design and transplantation. *Cell Transplant*. 2009;18(1):1–12.
21. Chen SZ, Ning LF, Xu X, et al. The miR-181d-regulated metalloproteinase Adamts1 enzymatically impairs adipogenesis via ECM remodeling. *Cell Death Differ*. 2016. doi:10.1038/cdd.2016.66
22. Sanders MA, Basson MD. Collagen IV regulates Caco-2 cell spreading and p130Cas phosphorylation by FAK-dependent and FAK-independent pathways. *Biol Chem*. 2008;389(1):47–55. doi:10.1515/BC.2008.008
23. Viale-Bouroncle S, Gosau M, Morsczeck C. Collagen I induces the expression of alkaline phosphatase and osteopontin via independent activations of FAK and ERK signalling pathways. *Arch Oral Biol*. 2014;59(12):1249–1255. doi:10.1016/j.archoralbio.2014.07.013
24. Pugacheva EN, Roegiers F, Golemis EA. Interdependence of cell attachment and cell cycle signaling. *Curr Opin Cell Biol*. 2006;18(5):507–515. doi:10.1016/j.ceb.2006.08.014
25. Kim MJ, Lee TH, Kim SH, et al. Triptolide inactivates Akt and induces caspase-dependent death in cervical cancer cells via the mitochondrial pathway. *Int J Oncol*. 2010;37(5):1177–1185.
26. Guo YM, Sun MX, Li J, et al. Association of CELF2 polymorphism and the prognosis of nasopharyngeal carcinoma in southern Chinese population. *Oncotarget*. 2015;6(29):27176–27186. doi:10.18632/oncotarget.4870
27. Xia YY, Yin L, Jiang N, et al. Downregulating HMGA2 attenuates epithelial-mesenchymal transition-induced invasion and migration in nasopharyngeal cancer cells. *Biochem Biophys Res Commun*. 2015;463(3):357–363.
28. Chen Y, Sun Y, Liang SB, et al. Progress report of a randomized trial comparing long-term survival and late toxicity of concurrent chemoradiotherapy with adjuvant chemotherapy versus radiotherapy alone in patients with stage III to IVB nasopharyngeal carcinoma from endemic regions of China. *Cancer*. 2013;119(12):2230–2238. doi:10.1002/cncr.28049
29. Hino N, Ichikawa T, Kimura Y, et al. An amphipathic helix of vinexin alpha is necessary for substrate stiffness-dependent conformational change in vinculin. *J Cell Sci*. 2018
30. Gaggioli C, Hooper S, Hidalgo-Carcedo C, et al. Fibroblast-led collective invasion of carcinoma cells with differing roles for RhoGTPases in leading and following cells. *Nat Cell Biol*. 2007;9(12):1392–1400. doi:10.1038/ncb1658
31. Bhuvanesh T, Machatschek R, Lysyakova L, et al. Collagen type-IV Langmuir and Langmuir-Schafer layers as model biointerfaces to direct stem cell adhesion. *Biomed Mater*. 2018
32. Bae YH, Mui KL, Hsu BY, et al. A FAK-Cas-Rac-lamellipodin signaling module transduces extracellular matrix stiffness into mechanosensitive cell cycling. *Sci Signal*. 2014;7(330):ra57. doi:10.1126/scisignal.2004838
33. Thiyagarajan V, Tsai MJ, Weng CF. Antroquinonol targets FAK-signaling pathway suppressed cell migration, invasion, and tumor growth of C6 glioma. *PLoS One*. 2015;10(10):e0141285. doi:10.1371/journal.pone.0141285
34. Lu Q, Rounds S. Focal adhesion kinase and endothelial cell apoptosis. *Microvasc Res*. 2012;83(1):56–63. doi:10.1016/j.mvr.2011.05.003
35. Yang S, Wang L, Kong Q. Depression of focal adhesion kinase induces apoptosis in rat osteosarcoma OSR-6 cells in a caspase-dependent pathway. *Cell Biochem Biophys*. 2014;70(2):765–770. doi:10.1007/s12013-014-9979-3
36. Liu J, Liu S, Chen Y, et al. Functionalized self-assembling peptide improves INS-1 beta-cell function and proliferation via the integrin/FAK/ERK/cyclin pathway. *Int J Nanomedicine*. 2015;10:3519–3531. doi:10.2147/IJN.S80502